NUMERICAL STUDY OF UNSTEADY FLOW AND HEAT TRANSPORT IN A VERTICAL CYLINDRICAL CONTAINER

N. L. Bachev and A. A. Kozlov

UDC 532.529.2:536.24

Different approximate methods [1, 2] have been used to calculate the temperature stratification in containers when heat is supplied externally. These methods are based on a provisional separation of the total volume into different zones (the boundary layer near the lateral wall, the central region, and the mixing region near the free surface). The equations defining the problem are then simplified and solved separately in each region. The features of the flow field can be taken into account more completely by numerically solving the unsteadyequations of thermal convection, where no a priori assumptions are made about the structure of the flow [3, 4, 5].

In practical problems the dimensionless parameters describing the flow regime (such as the Grashof and Rayleigh numbers) have values corresponding to turbulent convection. In [6] an approach was given to the numerical modeling of turbulent natural convection. This approach is based on the two-dimensional unsteady equations of thermal convection in terms of the variable vorticity, stream function, and temperature. The method does not use any additional empirical information. The numerical modeling in this approach involves the calculation of the intantaneous values of the required quantities by means of a finite-difference scheme based on a nonuniform grid, and a subsequent statistical analysis to find the average quantities and the characteristics of the fluctuations. This method can be used to study convection in a cylindrical container for Grashof numbers up to $1 \cdot 10^{13}$ and dimensionless times up to $t\nu/R^2 = 2.1 \cdot 10^{-3}$ [3, 4]. Further increases in the Grashof number and time lead to a violation of the stability and convergence requirements and the resulting numerical solution does not satisfy the conservation laws.

In the present paper we consider the numerical solution of the unsteady equations of thermal convection in terms of the velocity, pressure, and temperature. We use the control volume method. The temperature and velocity fields are calculated for the case of turbulent convection without the use of additional empirical information and the results are valid for sufficiently large values of the time.

1. Statement of the Problem. We consider unsteady natural convection in a partially filled vertical cylindrical container. The free surface of the liquid is assumed to be flat in the absence of frictional effects. Constant, uniformly distributed heat fluxes are applied to the lateral surface of the container, free surface of the liquid, and the bottom. The velocity and temperature fields are assumed to be axisymmetric and the angular component of the velocity is zero. The liquid is at rest at the initial time and has a constant temperature, which is taken as the reference point.

The equations of convection in cylindrical coordinates are written as:

$$\frac{1}{r}\frac{\partial}{\partial r}(r\rho V_r)+\frac{\partial}{\partial z}(\rho V_z)=0, \tag{1}$$

$$\frac{\partial(\rho V_r)}{\partial t}+\frac{1}{r}\frac{\partial}{\partial r}(r\rho V_r V_r)+\frac{\partial}{\partial z}(\rho V_r V_z)=-\frac{\partial P}{\partial r}+\frac{1}{r}\frac{\partial}{\partial r}\left(r\mu\frac{\partial V_r}{\partial r}\right)+\frac{\partial}{\partial z}\left(\mu\frac{\partial V_r}{\partial z}\right)+$$
$$+\frac{1}{r}\frac{\partial}{\partial r}\left(r\mu\frac{\partial V_r}{\partial r}\right)+\frac{\partial}{\partial z}\left(\mu\frac{\partial V_z}{\partial r}\right)-2\mu\frac{V_r}{r^2}, \tag{2}$$

$$\frac{\partial(\rho V_z)}{\partial t}+\frac{1}{r}\frac{\partial}{\partial r}(r\rho V_r V_z)+\frac{\partial}{\partial z}(\rho V_z V_z)=-\frac{\partial P}{\partial z}+$$
$$+\frac{1}{r}\frac{\partial}{\partial r}\left(r\mu\frac{\partial V_z}{\partial r}\right)+\frac{\partial}{\partial z}\left(\mu\frac{\partial V_z}{\partial z}\right)+\frac{1}{r}\frac{\partial}{\partial r}\left(r\mu\frac{\partial V_r}{\partial r}\right)+\frac{\partial}{\partial z}\left(\mu\frac{\partial V_z}{\partial z}\right)-\rho g, \tag{3}$$

Translated from Inzhenerno-Fizicheskii Zhurnal, Vol. 54, No. 3, pp. 398-405, March, 1988. Original article submitted October 27, 1986.

0022-0841/88/5403-0267$12.50

$$\frac{\partial(\rho cT)}{\partial t}+\frac{1}{r}\frac{\partial}{\partial r}(r\rho V_r cT)+\frac{\partial}{\partial z}(\rho V_z cT)=\frac{1}{r}\frac{\partial}{\partial r}\left(r\lambda\frac{\partial T}{\partial r}\right)+\frac{\partial}{\partial z}\left(\lambda\frac{\partial T}{\partial z}\right), \tag{4}$$

$$\rho=\rho_0[1-\beta(T-T_0)]. \tag{5}$$

Because of the axial symmetry of the convective flow field and temperature field, the solution can be calculated in the plane $0 \leq r \leq R$, $0 \leq z \leq H$. We next determine the initial and boundary conditions.

On the lateral surface and bottom of the container the no-slip condition is assumed, i.e., the normal and tangential components of the velocity vanish

$$V_r(r=R)=V_z(r=R)=V_r(z=0)=V_z(z=0)=0. \tag{6}$$

The following conditions apply on the symmetry axis and on the free surface of the liquid, reflecting the condition that the fluid cannot penetrate the surface and the absence of tangential stress:

$$V_r(r=0)=\frac{\partial V_z}{\partial r}(r=0)=V_z(z=H)=\frac{\partial V_r}{\partial z}(z=H)=0. \tag{7}$$

At the initial time t = 0 the liquid is at rest and it has a given initial temperature

$$t\leqslant 0 \quad V_r(r,z)=V_z(r,z)=0;\ T(r,z)=T_0. \tag{8}$$

During the time interval t_k constant heat fluxes exist through the lateral surface and bottom of the container and through the free surface:

$$0\leqslant t\leqslant t_k \quad q(r=R)=q_w;\ q(z=0)=q_D;\ q(z=H)=q_s. \tag{9}$$

The heat flux vanishes on the symmetry axis

$$0\leqslant t\leqslant t_k \quad q(r=0)=0. \tag{10}$$

2. Method of Solution. Study of the differential equations (2) through (4) shows that the dependent variables obey the generalized conservation law [7]:

$$\frac{\partial}{\partial t}(\rho\Phi)+\frac{1}{r}\frac{\partial}{\partial r}(r\rho V_r\Phi)+\frac{\partial}{\partial z}(\rho V_z\Phi)=\frac{1}{r}\frac{\partial}{\partial r}\left(r\Gamma\frac{\partial\Phi}{\partial r}\right)+\frac{\partial}{\partial z}\left(\Gamma\frac{\partial\Phi}{\partial z}\right)+S. \tag{11}$$

Four terms appear in (11): the unsteady, convective, diffusion, and source terms. The explicit forms of the coefficient of diffusion Γ and the source term S depend on the nature of the variable Φ. They have been determined for each of the dependent variables and are written out in Table 1. The components of the velocity are determined with respect to a grid shifted from the basic computational grid [7, 8], as shown in Fig. 1.

Introducing the convection-diffusion fluxes

$$J_r=r\left(\rho V_r\Phi-\Gamma\frac{\partial\Phi}{\partial r}\right);\ J_z=\rho V_z\Phi-\Gamma\frac{\partial\Phi}{\partial z}$$

and integrating (11) over a control volume (i, j), we obtain

$$\frac{\rho r_i\Delta r_i\Delta z_j(\Phi_{i,j}^{n+1}-\Phi_{i,j}^{n})}{\Delta t}+(J_3)_{i,j}^{n+1}-(J_1)_{i,j}^{n+1}+(J_4)_{i,j}^{n+1}-(J_2)_{i,j}^{n+1}=r_i\Delta r_i\Delta z_j[(S_c)_{i,j}^{n}+(S_p)_{i,j}^{n}\Phi_{i,j}^{n+1}], \tag{12}$$

where the source term is linearized according to the equation

$$S_{i,j}^{n+1}=(S_c)_{i,j}^{n}+(S_p)_{i,j}^{n}\Phi_{i,j}^{n+1}.$$

In a similar way we integrate the equation of continuity (1):

$$(F_3)_{i,j}^{n+1}-(F_1)_{i,j}^{n+1}+(F_4)_{i,j}^{n+1}-(F_2)_{i,j}^{n+1}=0. \tag{13}$$

Solving (12) and (13) simultaneously, we obtain the discrete analog of the generalized equation:

TABLE 1. Diffusion Coefficients and Source Terms in the Generalized Conservation Law

Φ	Γ_Φ	S_Φ
V_r	μ	$-\frac{\partial P}{\partial r}+\frac{1}{r}\frac{\partial}{\partial r}\left(r\mu\frac{\partial V_r}{\partial r}\right)+\frac{\partial}{\partial z}\left(\mu\frac{\partial V_z}{\partial r}\right)-2\mu\frac{V_r}{r^2}$
V_z	μ	$-\frac{\partial P}{\partial z}+\frac{1}{r}\frac{\partial}{\partial r}\left(r\mu\frac{\partial V_r}{\partial z}\right)+\frac{\partial}{\partial z}\left(\mu\frac{\partial V_z}{\partial z}\right)+\rho_0\beta(T-T_0)g$
T	$\frac{\lambda}{c}$	0

$$\alpha_{i,j}\Phi_{i,j}^{n+1}=(\alpha_1)_{i,j}\Phi_{i-1,j}^{n+1}+(\alpha_2)_{i,j}\Phi_{i,j-1}^{n+1}+(\alpha_3)_{i,j}\Phi_{i+1,j}^{n+1}+(\alpha_4)_{i,j}\Phi_{i,j+1}^{n+1}+B_{i,j}, \tag{14}$$

where

$$\alpha_1=D_1A(|\mathrm{Pe}_1|)+[|F_1,\ 0|];\quad \alpha_2=D_2A(|\mathrm{Pe}_2|)+[|F_2,\ 0|];$$
$$\alpha_3=D_3A(|\mathrm{Pe}_3|)+[|-F_3,\ 0|];\quad \alpha_4=D_4A(|\mathrm{Pe}_4|)+[|-F_4,\ 0|];$$
$$\mathrm{Pe}=\frac{F}{D};\quad A(|\mathrm{Pe}|)=[|0,\ (1-0{,}1\,|\mathrm{Pe}|)^5|];$$
$$\alpha_{i,j}=(\alpha_1+\alpha_2+\alpha_3+\alpha_4)_{i,j}+r_i\Delta r_i\Delta z_j\left[\frac{\rho}{\Delta t}-(S_p)_{i,j}\right];$$
$$B_{i,j}=r_i\Delta r_i\Delta z_j\left[(S_c)_{i,j}+\frac{\rho\Phi_{i,j}}{\Delta t}\right].$$

The discrete analogs express the laws of conservation of mass, energy, and momentum for a finite control volume in the same way as the original differential equations express the conservation laws for an infinitely small control volume. One of the important features of the control volume method is that the exact integral conservation laws of mass, energy, and momentum apply to an arbitrary group of control volumes, and not only to the limiting case of a very large number of them.

The calculations on the system of nonlinear equations (1) through (5) with the initial and boundary conditions (6) through (10) are done in the following order. For each time step the temperature field is determined and then the resulting convective flow field is calculated. We first determine an intermediate velocity field (V_r*, V_z*) without the effect of pressure forces taken into account. This intermediate velocity fields does not satisfy the equation of continuity. We calculate the mass imbalance $\Delta m_{i,j}$ for each cell, which is then used in the equation for the pressure correction:

$$\alpha_{i,j}P_{i,j}^{n+1}=(\alpha_1)_{i,j}P_{i-1,j}^{n+1}+(\alpha_2)_{i,j}P_{i,j-1}^{n+1}+(\alpha_3)_{i,j}P_{i+1,j}^{n+1}+(\alpha_4)_{i,j}P_{i,j+1}^{n+1}+\Delta m_{i,j}. \tag{15}$$

Then the solution of the discrete equation (15) is used to correct the intermediate velocity field (V_r*, V_z*) and thereby obtain the actual velocity field (V_r, V_z), which satisfies the equation of continuity. The entire procedure is repeated for each subsequent time step.

3. Numerical Results and Comparison with Experiment. We use dimensionless quantities, where the scales of length, time, temperature, and velocity are given by H, H^2/ν, q_wH/λ, ν/H, respectively.

We performed a series of calculations using different methods of solving the discrete analogs of the equation of motion, and the temperature and pressure equations. We tried the method of successive highest relaxation, and the method of variable direction. These iterative methods gave good convergence for the solutions of the velocity and temperature equations but the convergence was very slow for the solution of the pressure correction equation. The

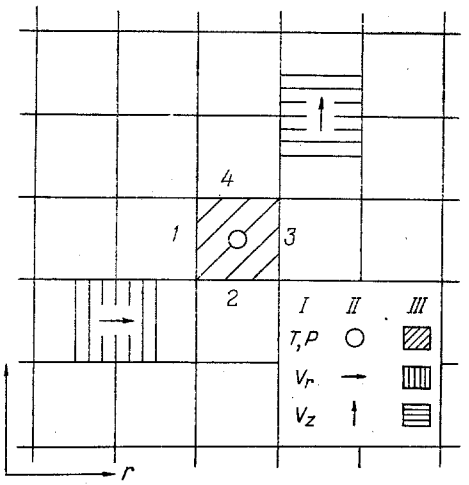

Fig. 1. Computational grid: I) variables, II) notation, III) volume.

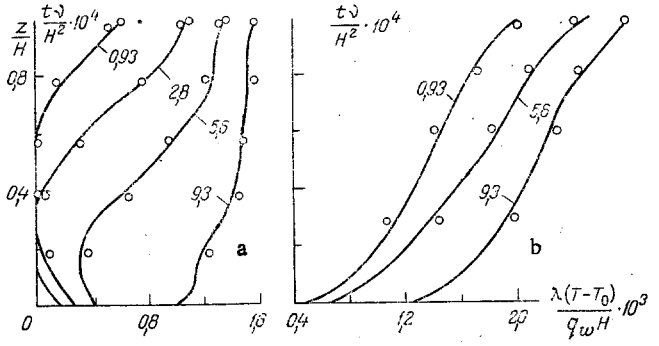

Fig. 2. Vertical temperature profile at a distance r/H = 0.075 from the axis (a) and Δr/H = 0.003 from the lateral wall (b) (dimensionless units).

results shown in Figs. 2-4 were obtained using the method of elimination. Calculations were done for different values of the Grashof number $Gr = g\beta q_w H^4/\lambda\nu^2$ and dimensionless time $\tau = t\nu/H^2$ with the use of various time and spatial stepsizes. The program used a nonuniform grid in the spatial coordinates in order to obtain the best resolution of the fields in regions where the gradients of the variables were large. The following systems of cells were used: 10 × 10, 15 × 15, 20 × 20, 25 × 25. The results discussed below were obtained for a 15 × 15 grid. Use of different time steps Δτ from $3.1\cdot10^{-7}$ to $5.6\cdot10^{-4}$ showed that the model gives stable results for all values of Δτ considered. However, good agreement between the calculated and experimental data is obtained with $\Delta\tau = 1.9\cdot10^{-5}$. Large values of Δτ lead to relatively large variations in the velocity and temperature fields during a single time step and this causes significant disagreement between the calculated and experimental data. The results shown in Figs. 2-4 were obtained using $\Delta\tau = 3.1\cdot10^{-6}$.

In the experiments, water was chosen as the working liquid. A vertical container of diameter 0.8 m was partially filled up to a height of 1.8 m. The walls and bottom of the cylinder were made of steel of thickness 0.005 m. External heat fluxes were created by heating the surrounding air with a heating element. Chromel–Copel thermocouples were used as temperature detectors. The thermocouples were connected to an automated system and the experimental data was analyzed on the microcomputer DZ-28. The error of the temperature meter was 1.6%. Readings were taken from the thermocouples every 60 sec.

The distribution of temperature with height in the liquid was measured at a distance r/H = 0.075 from the axis of the container by means of eight thermocouples mounted on a probe. In order to obtain the best resolution of the temperature profile near the free surface of the liquid, six thermocouples were mounted on a float. The temperatures of the inner and outer surfaces of the container were measured with thermocouples distributed over the entire height of the lateral surface and over the entire radius of the bottom of the container and were

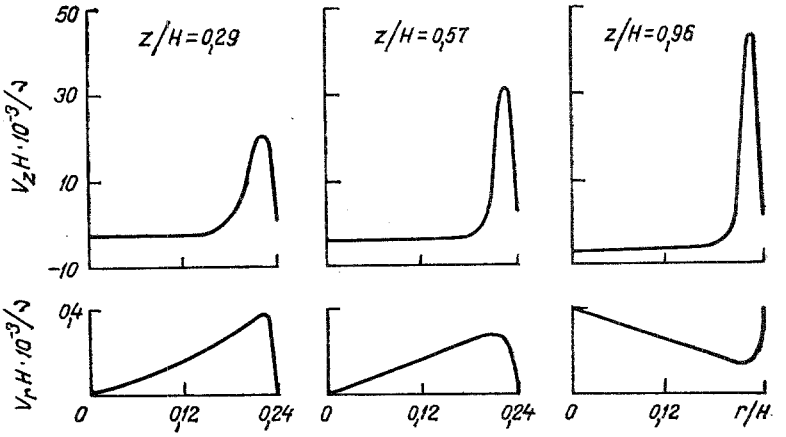

Fig. 3. Variation of the velocity components with radius (dimensionless quantities).

placed on the inner and outer surfaces. Six thermocouples were placed at a distance $\Delta r/H = 0.003$ from the lateral wall in order to measure the vertical temperature profile near the wall. The temperature of the surrounding air near the lateral wall, bottom, and above the free surface was also measured. Using the measured temperatures, the heat fluxes into the liquid through the lateral surface, bottom, and free surface were calculated:

$$q_w(z, \tau) = A_a(T_a - T_w)^{4/3},$$
$$q_D(r, \tau) = A_a(T_a - T_D)^{4/3},$$
$$q_s(r, \tau) = A_a(T_a - T_s)^{4/3},$$

where $A_a = (g\beta c_p \lambda^2 \rho^2/\mu)_a$ [9].

Then the heat fluxes were averaged over time and the coordinates and these average values were used in the further calculations. Figure 2 shows the calculated and experimental temperature profiles in the liquid at different times. The experimental data is denoted by the open circles. The temperatures are expressed as deviations from the initial temperature. The results shown are for the Rayleigh number $Ra = 3 \cdot 10^{13}$, and $q_D/q_w = 1$, $q_s/q_w = 0.9$. The maximum deviation between the calculated and experimental data was 3.2%. The temperature of the surface of the liquid was higher than the temperature of the liquid at the bottom of the container both near the axis of the container and near the lateral wall, even though $q_s < q_D$. This is due to convective transport of heat by means of flow of hot liquid toward the liquid–gas surface.

Figure 3 shows the radial dependence of the velocity components at three horizontal cross sections of the container for the time $\tau = 9.3 \cdot 10^{-4}$ and $Ra = 3 \cdot 10^{13}$. It is evident that due to the effect of the external heat fluxes, liquid at the wall is lifted upward, while backflow is observed immediately outside the boundary layer. The maximum velocity is different in different horizontal cross sections; it increases as one approaches the free surface.

Figure 4 shows the lines of constant excess temperature at the time $\tau = 9.3 \cdot 10^{-4}$ for $Ra = 3 \cdot 10^{13}$. Curves 1 and 2 correspond to the isotherms $1.244 \cdot 10^{-3}$ and $1.493 \cdot 10^{-3}$, respectively. A steep drop in the curves is observed near the temperature boundary-layer, and the drop becomes steeper with increasing time. The isotherms are nearly horizontal outside of the boundary layer and the temperature increases as one moves in the vertical direction.

For dimensionless times larger than $9.3 \cdot 10^{-4}$ a significant disagreement is observed between the calculated and experimental data. This can be explained as follows. When additional empirical information is not used in the numerical modeling of turbulent natural convection, we neglect all motion on a scale smaller than the cell size. Therefore it is evident that the energy needed to maintain these subcell fluctuations is not taken into account in the calculation. Hence the numerical method given here is only valid over time intervals that are sufficiently small. However, the time interval over which the calculation is valid is large enough to be of interest for many practical problems.

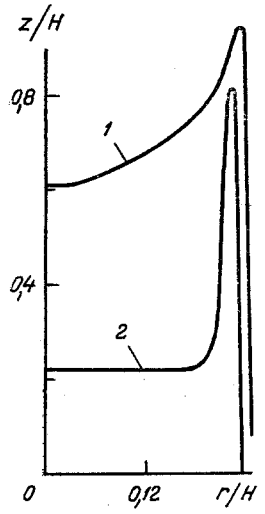

Fig. 4. Excess temperature isotherms (dimensionless quantities).

In summary, we have presented a numerical model to predict the temperature field in a liquid which partially fills a vertical cylindrical container in the case of turbulent natural convection. The method does not make use of additional empirical information and is based on approximating the conservation laws of mass, momentum, and energy by discrete equations in time and space, and the integration of these equations over control volumes and a certain time interval. The use of different grids makes it possible to obtain stable numerical results for large values of the regime parameters and sufficiently large values of the time and the results closely agree with experimental data.

NOTATION

Gr, Grashof number; Pr, Prandtl number; Ra, Rayleigh number; t, time; τ, dimensionless times; r, z, cylindrical coordinates; V_r, V_z, radial and vertical components of the velocity; P, pressure; T, temperature; T_0, initial temperature; μ, dynamical viscosity; c, specific heat; λ, thermal conductivity; ρ, density; ρ_0, density corresponding to the initial temperature; β, coefficient of thermal expansion; g, acceleration of gravity; ν, kinematic viscosity; R, radius of the cylinder; H, height of the liquid in the container; q, heat flux; Φ, generalized variable; Γ, coefficient of diffusion; S, source term; J, convection-diffusion flux; i, j, indices numbering the control cells; Δr, Δz, cell dimensions along the r and z directions; n, number of time steps; Δt, time stepsize; S_c, S_p, coefficients in the linearization of the source; F, mass flow rate; D, conductance; Pe, Peclet number; [A, B], the larger of the two quantities A and B. Indices: a, air; w, wall; D, bottom; s, free surface.

LITERATURE CITED

1. D. A. Clark, "Cryogenic heat transfer," Advances in Heat Transfer [Russian translation], Moscow (1971), pp. 361-567.
2. V. F. Khlybov, Khim. Petr. Mash., No. 5, 16-17 (1978).
3. V. I. Polezhaev and S. G. Cherkasov, Izv. Akad. Nauk SSSR, Mekh. Zhidk. Gaza, No. 4, 148-157 (1983).
4. S. G. Cherkasov, Izv. Akad. Nauk SSSR, Mekh. Zhidk. Gaza, No. 6, 51-56 (1984).
5. N. L. Bachev and A. A. Kozlov, Izv. Vyssh. Uchebn. Zaved., Aviats. Tekh., No. 3, 13-17 (1985).
6. A. G. Daikovskii, V. I. Polezhaev, and A. I. Fedoseev, "Numerical modeling of transitional and turbulent convection on the basis of the unsteady Navier—Stokes equations," Preprint IAM (IPM), Acad. of Sciences of the USSR, Moscow (1978).
7. S. Patanker, "Numerical methods of solution of problems of heat exchange and the dynamics of liquids," Translated from English by V. D. Vilenskii, Moscow (1984).
8. N. Markatos and M. Malin, Int. J. Heat Mass Transfer., 2, No. 1, 63-75 (1982).
9. S. S. Kutateladze and V. M. Borishanskii, Handbook of Heat Transfer [in Russian], Leningrad—Moscow (1959).